The Influence of Slope Geometry on its Stability: Spatial and Plane Analysis

Lesław Zabuski

Institute of Hydro-Engineering, Polish Academy of Sciences, 7 Kościerska, 80-328 Gdańsk, Poland,
e-mail: leslawzabuski@ibwpan.gda.pl

Abstract

The paper presents the results of numerical calculations of the stability and deformation process of several idealized slopes performed by the elasto-plastic finite difference method, using the commercial codes FLAC3D and FLAC2D. The results of 3D analysis of these slopes are compared with those obtained by the 2D method. The behaviour of slopes of different shapes and inclinations was analyzed. The calculations were carried out for flat, concave and convex slopes inclined at 30°, 45° and 60°, taking into account the influence of the lateral constraints of the slope. Two variants of the medium were analysed, i.e. the mass with no friction and with no cohesion. A comparison of 3D calculation results with those obtained by the 2D limit equilibrium analysis indicates that the 3D approach produces almost always higher safety factors than does the 2D method.

Key words: slope stability, landslide, spatial analysis, numerical calculations, deformation process

1. Introduction

Recently, there has been a significant increase in the use of three-dimensional (3D) numerical methods for establishing the stability of slopes. The advantages of the 3D methods over the 2D approach to analyzing the stability of slopes are well recognized (Griffith and Marquez 2007; Zabuski 2005). The present paper reports the results of a 3D analysis of the influence of slope morphology on its stability conditions. Deformation processes were simulated by the computer code FLAC3D (Itasca 1997), based on the finite difference method for calculations of the stress and strain distribution (Chugh 2003). Stability was also analyzed for the plane (2D) model of the slope, i.e. in a plane strain state. The results obtained by these two approaches were compared, and conclusions were drawn with regard to the safety factors obtained by the 2D and 3D methods.

Several authors have compared the results of 3D analyses with those obtained by 2D analyses (Bromhead and Martin 2004, Chang 2002, Chen and Chameau 1982,

Farzaneh and Askari 2003, Huang et al 2002, Hungr et al 1989, Lam and Fredlund 1993, Zhang 1988, Stark and Eid 1998). Safety factors computed in 3D trials are almost universally higher than those obtained by the 2D analysis (Hutchinson and Sarma 1985, Hungr 1987), unless the medium is heterogeneous (e.g. Duncan 1996, Arellano and Stark 2000).

The schemes of slopes built of an isotropic elasto-ideally plastic medium, which obeys the Coulomb-Mohr criterion and a non-associated flow rule, were analyzed (Zabuski 2002). The lateral walls of the models were either fixed or constrained by the assumption of their high strength parameters. In addition, the behaviour of the slopes was investigated in two "idealized" variants. The first one assumed a non-cohesive medium (e.g. sand-like soil), while in the second variant the angle of friction was equal to zero (e.g. clay).

The 3D models of slopes analyzed in this paper are comparable to real objects built of softened rock/soil mass. Landslides develop in zones of tectonic disturbances (e.g. faults, fault zones). The tectonically disturbed (softened) zones are usually loose and fragmented, whereas the surrounding massif tends to have better geomechanical properties. Therefore it seems that the idealized models adequately represent natural slopes, at least to some extent.

2. Models of Slopes

The following models of slopes were analyzed:
 – flat wide (Fig. 1A),
 – flat narrow (Fig. 1B),
 – concave – constrained lateral walls (Fig. 2A),
 – concave – arch (Fig. 2B),
 – convex – arch (Fig. 3A),
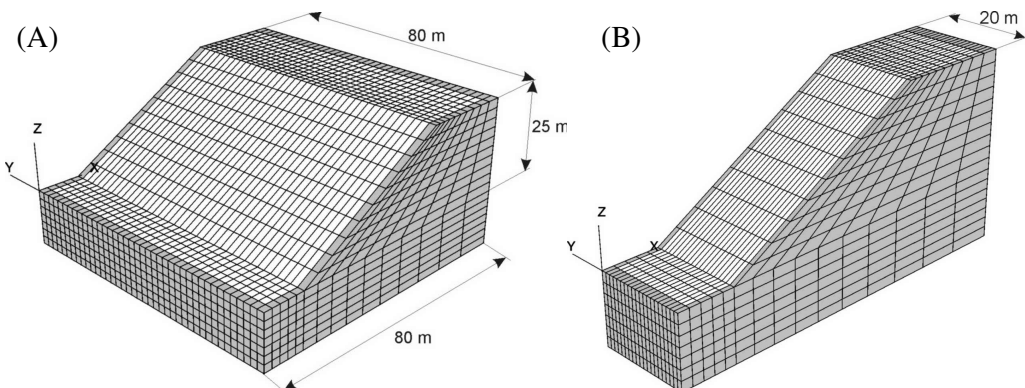 – convex – arch, constrained lateral walls (Fig. 3B).
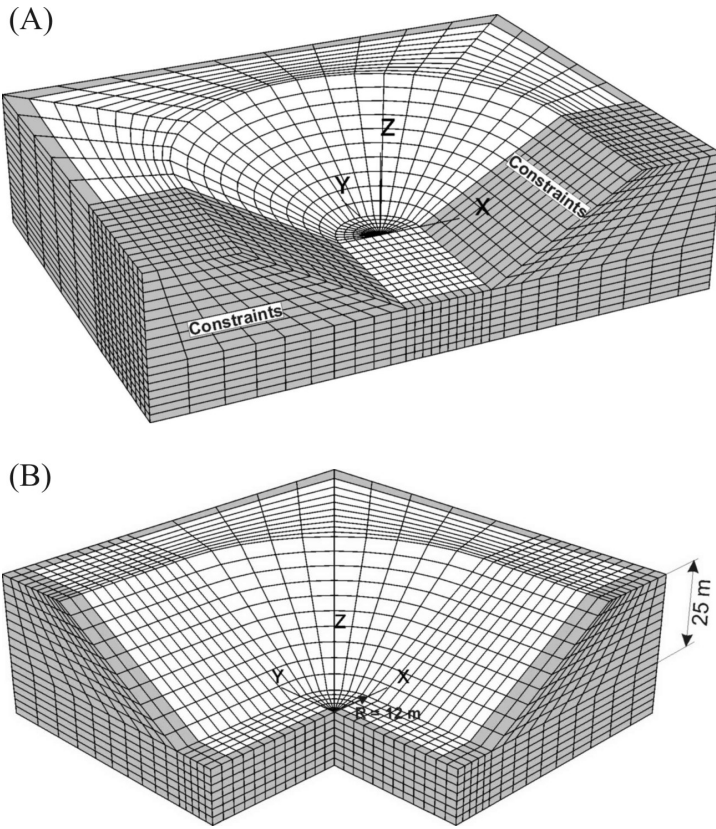

Fig. 1. Flat slope; (A) wide, (B) narrow

(A)

(B)

Fig. 2. Concave slope; (A) with constrained lateral walls, (B) with constraints of lateral walls
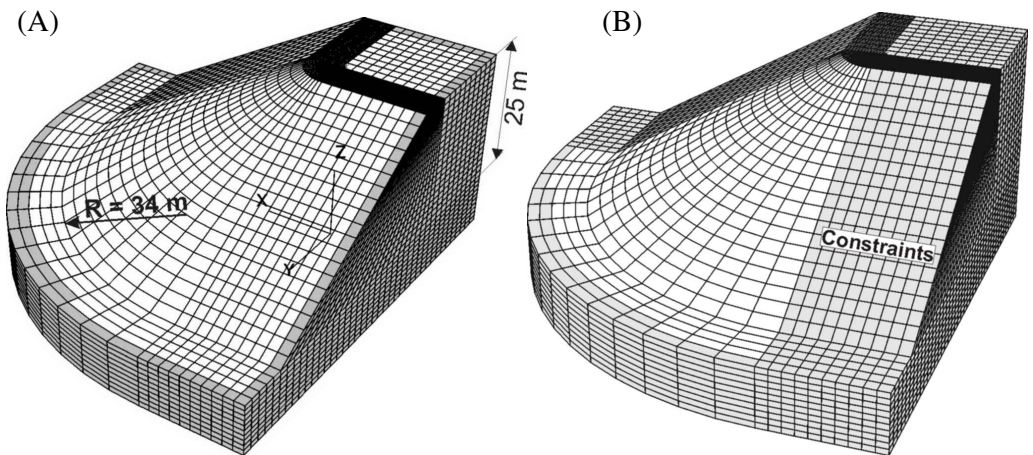
(A)

(B)

Fig. 3. Convex slope; (A) without constraints of lateral walls, (B) with constrained lateral walls

Slope inclinations of 30°, 45° and 60° were analysed for each of the above-mentioned models (the figures show slopes inclined at 30°). The limited values of the angle of friction and cohesion were calculated for each of the models. These values were compared with those calculated for the remaining models and with parameters determined by 2D calculations using FLAC2D (Itasca 2000).

The medium composing the slopes is isotropic, homogeneous and elasto-ideally plastic with the following parameters:
- elasticity modulus E = 10 MPa,
- Poisson's coefficient v = 0.35,
- tension strength = 50% × cohesion,
- non-associated flow rule, dilatation angle = 25% × friction angle.

The numerical analysis aimed to establish the limited values of cohesion and the angle of friction, i.e. the values corresponding to the limited state of stability (where F = 1.0).

3. Calculation Results: Presentation and Discussion

Table 1 shows the values representing cohesion and the angle of friction corresponding to the limited state of stability for the different slopes analyzed.

Table 1. Limit values of the shear strength parameters

| Lp.	Slope model	Slope inclination [°]	Cohesion c [kPa]	Angle of friction Φ [°]
1	2D model	30	79–80	30
		45	86–87	44–44.5
		60	98–99	56–57
2	Flat wide	30	59–60	29–29.5
		45	70–71	40–40.5
		60	83–84	51–52
3	Flat narrow	30	34–35	28
		45	43–44	37–38
		60	52–52.5	44–45
4	Concave with constrained lateral walls	30	50–51	27–28
		45	55–56	36–37
		60	60–61	41–42
5	Concave	30	56	28.5–29
		45	64–65	40–40.5
		60	73–73.5	50–51
6	Convex	30	56	30–30.5
		45	51–52	43–44
		60	72–73	57–58
7	Convex with constrained lateral walls	30	42–43	29.5–30
		45	45.5–46	44–44.5
		60	65.5–66	57.5–58
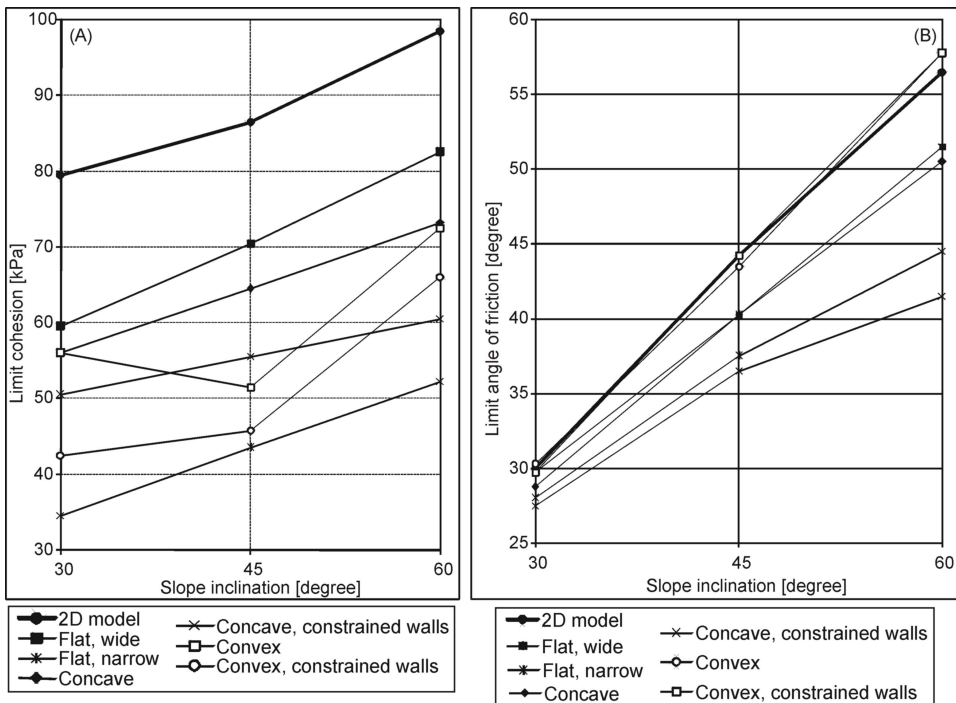
Fig. 4. Limit shear strength parameters as a function of the slope inclination (A) cohesion;
(B) angle of friction

Figures 4A and 4B present the limited values of cohesion and the angle of friction as a function of the slope inclination for all models. These diagrams make it possible to compare the conditions of stability loss in each of the variants tested. The higher the location of the curve, the larger the strength parameters necessary for assuring slope stability on the limit equilibrium level (Cavounidis 1987). The 2D slope turned out to be the least stable in the cases of both no cohesion and no angle of friction. The highest limited values of the angle of friction, close to Φ obtained by 2D calculations in the medium without cohesion, were determined for the convex slopes. The highest values of cohesion in the case of the medium without friction were determined for the flat wide slope, but they are significantly lower than the values from 2D calculations.

Figures 5A and 5B present the values of $(c_{2D} - c_{lim})/c_{lim}$ and $(\Phi_{2D} - \Phi_{lim})/\Phi_{lim}$ in ascending order for the slope models (shown on the horizontal axis). High values of these ratios indicate a more prominent influence of a three-dimensional shape of the slope and the constraints of lateral walls on the stability]. Differences emerged between the media without friction and without cohesion. In the case of no friction, the extent of displacement is large (Silvestri 2006): the landslides are extensive and deep. The impact of lateral constraints is considerable, whereas the significance of the shape of the slope is relatively smaller. In the case of no cohesion, the shape of the slope plays a more important role, with the convex and flat wide slopes being the
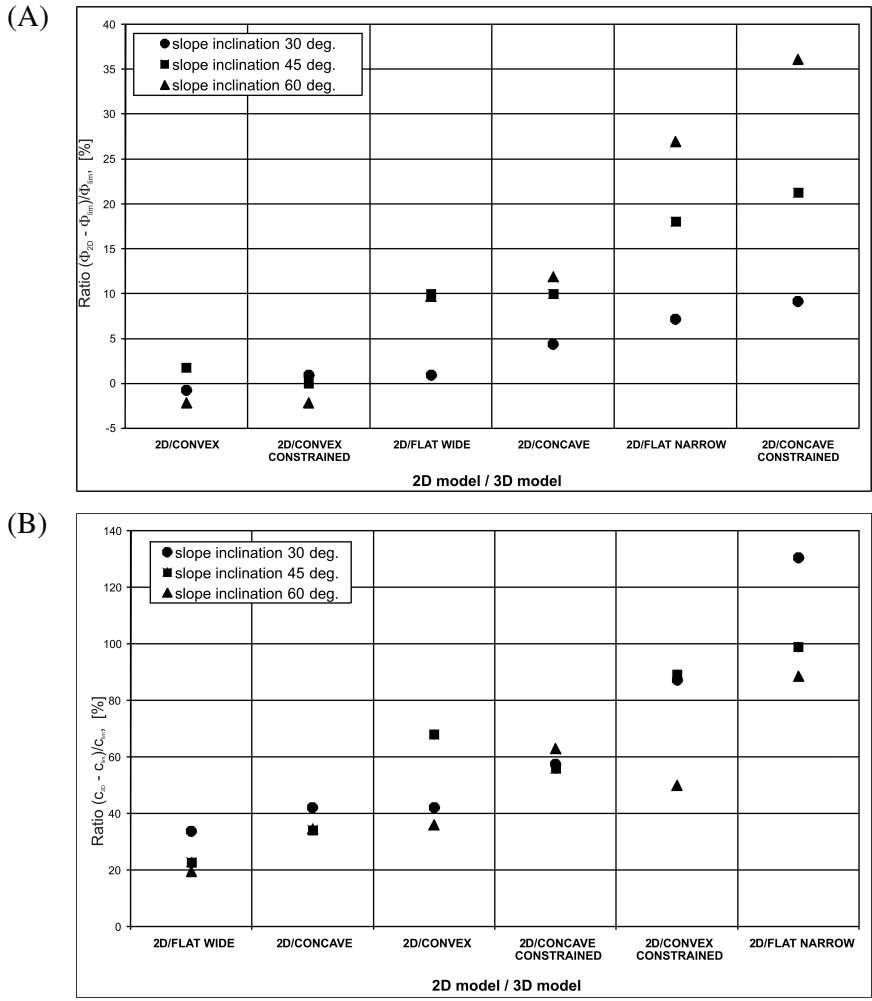
(A)

(B)

Fig. 5. Ratio of the shear parameters for the slope models analyzed (A) $(\Phi_{2D} - \Phi_{lim})/\Phi_{lim}$; (B) $(c_{2D} - c_{lim})/c_{lim}$

most prone to failure. The conditions conducive to the failure of concave slopes, but not of flat narrow slopes, suggest that the influence of lateral constraints cannot be ignored in the case of the non-cohesive medium either.

In addition, the differences between the limit values obtained in 2D and 3D analyses and between the slope shapes also depend on the slope inclination. In the cases of the non-cohesive medium, these differences are significant, and they are bigger for steeper slopes (see Fig. 5A). In the frictionless medium, the influence of the inclination is less prominent, and the dependence is different than in the non-cohesive case in that the differences are bigger for smaller slope inclinations (see Fig. 5B; c_{lim} and Φ_{lim} represent the limit values of these parameters, corresponding to the onset of the 3D model failure).

The failure mechanism is determined by the following factors:
– slope shape (flat, concave, convex);
– slope inclination;
– strength properties of the medium (non-cohesive, frictionless);
– lateral constraints of the slope.

While the slope shape is of minor importance in determining the failure mechanism, the impact of slope inclination is much more significant. In the non-cohesive medium, when the inclination is 60° or 45°, the dominant failure mechanism is toppling, and the typical slide occurs when the inclination is low (e.g. 30°, Fig. 6). In the case of a large inclination, the failure process is initiated in the uppermost part of the slope, and the process of deformation has a "local" character, affecting only a small part of the slope and leaving its lower part intact. If the inclination is smaller, the slide begins in the upper part and extends approximately to the slope base.

These results suggest that landslides on steep slopes rarely occur in the form of classical slides, and their extent is concentrated in the upper part of the slope and first of all have a toppling or rockfall character. The interpretation of the processes as phenomena embracing the whole slope (from the crown to the toe) is therefore incorrect in some cases.

The landslide processes in a highly cohesive medium unfold in a different way. The slip surface has an approximately circular shape and "runs" partially below the slope base. Its outcrops are in the toe region, where they create bulges (Fig. 7). Figures 7a–c present the bulges in a schematic way and Fig. 7d shows the example of very distinct natural bulge on the road at the toe of the landslide. Such phenomenon is the effect of the pressure exerted by the mass lying in the upper part of the slope. The extent of deformation in the flat region of the slope crown is the bigger, the smaller the slope inclination. In other words, the volume of the landslide depends on the slope inclination.

The landslide processes in masses without cohesion (e.g. loose debris, non-cohesive soil) occur at relatively shallow depths. The failure develops in a shear mode, whereas when the slope is steep, the failure occurs in a toppling mode. Slopes composed of massifs having large cohesion fail in the form of both slides and tension in the uppermost zones of the slope (Fig. 8).

The lateral constraints of slopes have a major impact on the stability conditions and failure mechanism. However, this influence depends on the slope shape and is most significant for convex slopes.

4. Summary and Conclusions

• The overall strength of the slope, representing its global resistance against the loss of stability, is higher (in some cases considerably) when computed by the 3D method than it is when calculated in two dimensions, i.e. under the plane strain conditions.
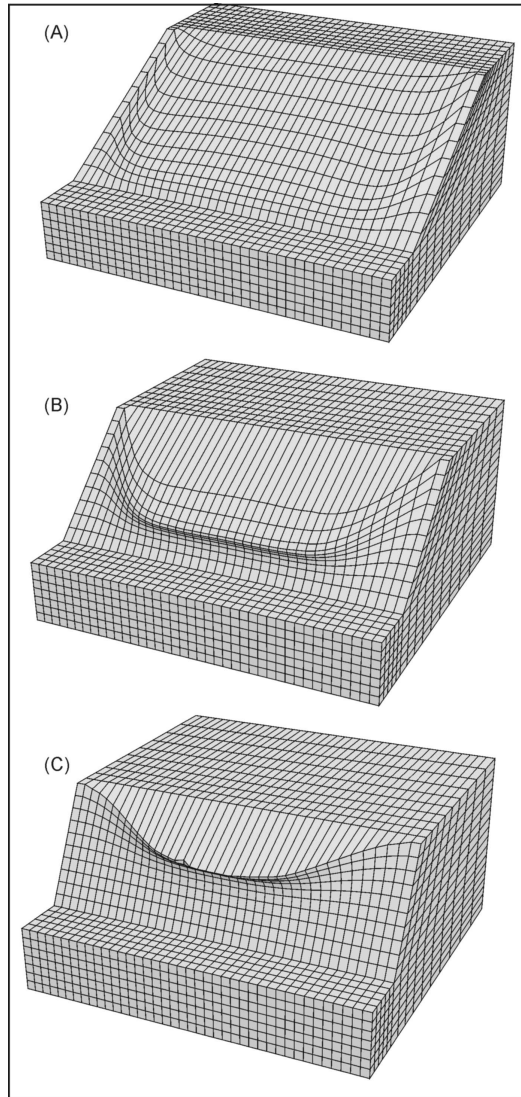
Fig. 6. Flat wide slope without cohesion; (A) inclination 30°, (B) inclination 45°;
(C) inclination 60°

- The shape of the slope (flat, concave, convex) and lateral constraints are major influences on its stability. Slopes with large constraints (e.g. flat narrow slopes) show the highest stability.
- The lowest safety factors in 3D calculations were obtained for the flat and wide slope. In this case, the distance between the lateral constraints is large and therefore their influence is small. This model is closest to the 2D model.
- Unlike slope stability, which depends on the slope shape and lateral constraints, the failure mechanism is mainly determined by the mass properties (material without
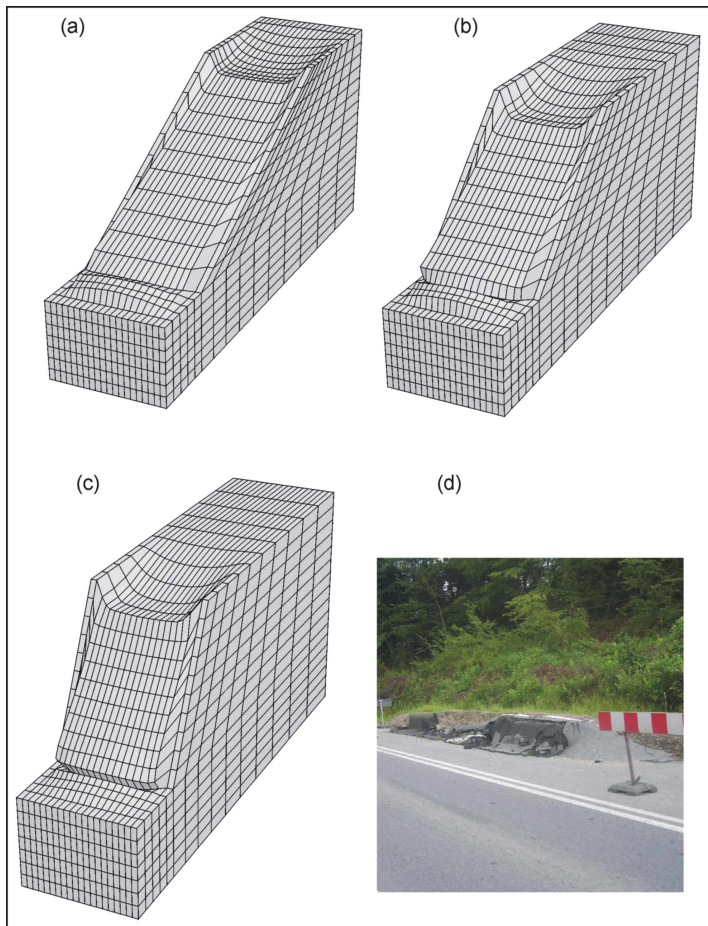
Fig. 7. Flat narrow slope without friction; (a) inclination 30°, (b) inclination 45°; (c) inclination 60°; (d) bulge on the road at the toe of the landslide
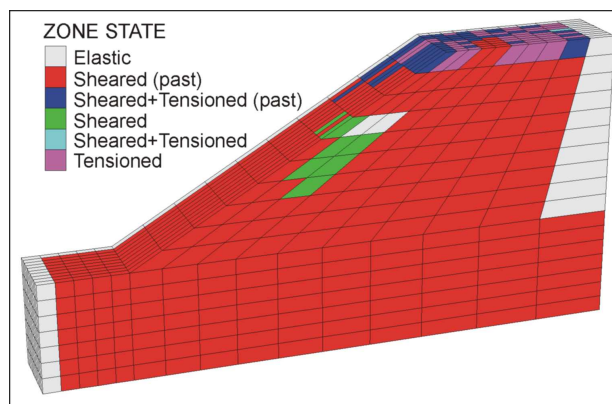

Fig. 8. Distribution of plasticity zones in a frictionless medium, slope inclination 30°

friction or cohesion) and the slope inclination (Zabuski et al 1999). If the slope is steep, toppling or rockfall in its upper part is the dominant mechanism of failure. If the inclination is smaller, classical slides occur (see Fig. 6). It could be estimated that the borderline between toppling and slide failures lies in the range between 35° and 40°.

- The depth of the deformation process in non-cohesive media is relatively small, and the landslides generated have a translational character. In frictionless media, deep rotational slides occur (Fig. 9). In the case of no cohesion, the main scarps are flat, whereas in the case of no friction, they are circular. Thus it is possible to estimate the character of the landslide on the basis of the shape of its main scarp.

- In the case of a shallow movement, the extent of the deformation zone is limited approximately to the upper half of the slope. The movement is initiated in the upper part of the slope, and the broken or sliding massif is accumulated in its lower part, covering the original, often intact, surface.

- Some conclusions emerging from the 3D analysis can also be drawn on the basis of 2D calculations, even those using simple material models and limit equilibrium methods. Nevertheless, the numerical calculations presented in this paper offer additional benefits, making it possible to identify crucial deformation processes that occur in nature (e.g. toppling or the creation of broken zones in the crown of the slope) (Bober et al 1997, Bober and Zabuski 1993). Such processes cannot be identified using the limit equilibrium method and the rigid-ideally plastic model of the medium.

- Three-dimensional analysis is more realistic than 2D solutions. It is more accurate and promotes a better understanding of the nature of the slope deformation and failure mechanism.
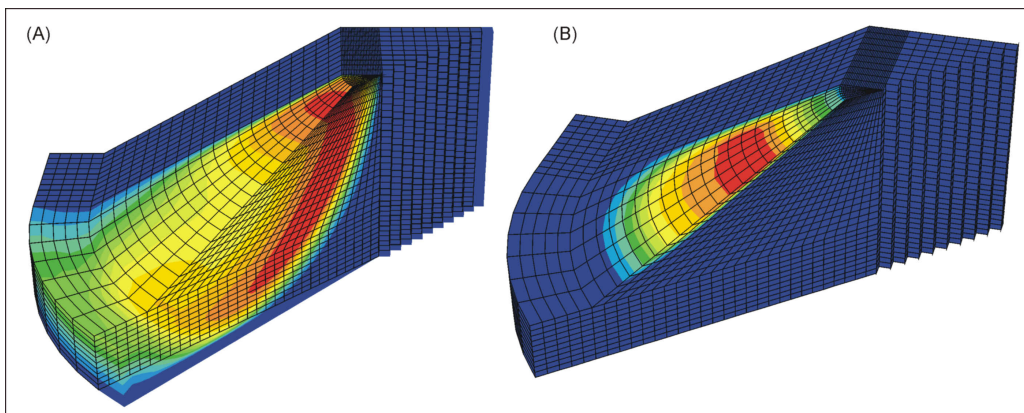

Fig. 9. Convex slope – the field of total displacement (A) medium without friction; (B) medium without cohesion

References

Arellano D., Stark T. D. (2000) Importance of three-dimensional slope stability analysis in practice, [in:] Griffiths D. V. et al (Editors), *Slope Stability 2000*, GSP No. 101, Reston, ASCE, 18–32.

Bober L., Thiel K., Zabuski L. (1997) *Zjawiska osuwiskowe w polskich Karpatach fliszowych – geologiczno-inżynierskie właściwości wybranych osuwisk*, IBW PAN, Gdańsk (in Polish).

Bober L., Zabuski L. (1993) Flysch Slope Classification from Viewpoint of the Landslide Prediction, *Proc. Int. Symp. Geotechnical Eng. of Hard Soils-Soft Rocks*, Athens, A.A. Balkema, Rotterdam-Brookfield, Vol. 2, 1965–1072.

Bromhead E. N., Martin P. L. (2004) Three-dimensional limit equilibrium analysis of the Taren landslide, [in:] *Advances in geotechnical engineering*, Thomas Telford, London, Vol. 2, 789–802.

Cavounidis S. (1987) On the ratio of factors of safety in slope stability analyses, *Geotechnique*, **37** (2), 207–210.

Chang M. (2002) A 3D slope stability analysis method assuming parallel lines of intersection and differential straining of block contacts, *Can. Geotech. J.*, **39** (4), 799–811.

Chen R. H., Chameau J. L. (1982) Three-dimensional limit equilibrium analysis of slopes, *Geotechnique*, **32** (1), 31–40.

Chugh A. K. (2003) On the boundary conditions in slope stability analysis, *Int. J. Numer. Anal. Methods Geomech.*, **27** (11), 905–926.

Duncan J. M. (1996) Soil slope stability analysis, [in:] Turner A. K. et al (Editors), *Landslides: Investigation and mitigation*, Special Report 247, Chapter 13. Washington, DC: Transportation Research Board, 337–371.

Farzaneh O., Askari F. (2003) Three-dimensional analysis of non-homogeneous slopes, *J. Geotech. Geoenviron. Eng.*, **129** (2), 137–145.

Griffiths D. V., Marquez R. M. (2007) Three-dimensional slope stability analysis by elasto-plastic finite elements, *Geotechnique*, **57** (6), 537–546.

Huang C. C., Tsai C. C., Chen Y. H. (2002) Generalized method for three-dimensional slope stability analysis, *J. Geotech. Geoenvironmental Eng. ASCE*, **128** (10), 836–848.

Hungr O. (1987) An extension of Bishop's simplified method of slope stability analysis to three dimensions, *Geotechnique*, **37** (1), 113–117.

Hungr O., Salgado F. M., Byrne P. M. (1989) Evaluation of three-dimensional method of slope stability analysis, *Can. Geotech. J.*, **26** (4), 679–686.

Hutchinson J. N., Sarma S. K. (1985) Discussion on "Threedimensional limit equilibrium analysis of slopes", *Geotechnique*, **35** (2), 215 p.

Itasca (1997) *FLAC 3D User's Manual*, Itasca Consulting Group, Minneapolis.

Itasca (2000) *FLAC 4.0 User's Manual*, Itasca Consulting Group, Minneapolis.

Lam L., Fredlund D. G. (1993) A general limit equilibrium model for three-dimensional slope stability analysis, *Can. Geotech. J.*, **30** (6), 905–Ő919.

Silvestri V. (2006) A three-dimensional slope stability problem in clay, *Can. Geotech. J.*, **43** (2), 224–228.

Stark T. D., Eid H. T. (1998) Performance of three-dimensional slope stability methods, *J. Geotech. Geoenviron. Eng.*, **124** (11), 1049–1060.

Zabuski L. (2002) Wpływ procedury wykonania zabiegów stabilizujących na stateczność podcinanego zbocza, *Materiały Konferencji "Stabilizacja masywów skalnych w podłożu budowli hydrotechnicznych"*, Żywiec 2002, IMGW Warszawa, 127–132 (in Polish).

Zabuski L. (2005) Numerical three-dimensional modeling of the landslide process in the Carpathian Flysch, *Int. Conf. "Mass Movement Hazard in Various Environments"*, 20–21.10.2005, Kraków, Polish Geological Institute, Centre of Excellence REA, Warsaw, 43–44.

Zabuski L., Thiel K., Bober L. (1999), *Osuwiska we fliszu Karpat polskich, Geologia-modelowanie-obliczenia stateczności*, IBW PAN, Gdańsk (in Polish).

Zhang X. (1988) Three-dimensional stability analysis of concave slopes in plain view, *J. Geotech. Eng. ASCE*, **114** (6), 658–671.